Available online at www.sciencedirect.com
SCIENCE DIRECT®
Journal of Organometallic Chemistry 691 (2006) 111–121
Journal of Organometallic Chemistry
www.elsevier.com/locate/jorganchem

Reactions of diphenylpyridylphosphine with $H_2Os_3(CO)_{10}$ and $H_4Ru_4(CO)_{12}$, P–C bond splitting in the coordinated ligand and isolation of the oxidative addition products

Vadim I. Ponomarenko [a], Tatiana S. Pilyugina [a,1], Vassily D. Khripun [a], Elena V. Grachova [a], Sergey P. Tunik [a,*], Matti Haukka [b], Tapani A. Pakkanen [b]

[a] *Department of Chemistry, St. Petersburg University, Universitetskii pr., 26, St. Petersburg, 198504, Russian Federation*
[b] *Department of Chemistry, University of Joensuu, P.O. Box 111, FIN-80101 Joensuu, Finland*

Received 24 June 2005; received in revised form 2 August 2005; accepted 3 August 2005
Available online 28 September 2005

Abstract

The reactions of diphenylpyridylphosphine ligand with $H_2Os_3(CO)_{10}$ and $H_4Ru_4(CO)_{12}$ were studied. It was found that the thermodynamic products of these reactions, (μ-H)$Os_3(CO)_9(\mu_3,\kappa^2$-PhP(2-$C_5H_4N$)) (**2**) and $H_3Ru_4(CO)_{10}(\mu_3,\kappa^2$-PhP(2-$C_5H_4N$)) (**4**), are formed through the oxidative addition of a P–Ph bond in the coordinated ligand and subsequent reductive elimination of benzene. In the case of triosmium cluster an unusually stable intermediate compound, (μ-H)$_2Os_3(CO)_8(\mu_3,\kappa^2$-PhP(2-$C_5H_4N$))(Ph) (**1**), containing *cis* hydride and σ-bonded phenyl was isolated and fully characterized. This cluster eliminates benzene to give (**2**) only under heating above 50 °C. Reaction of $H_4Ru_4(CO)_{12}$ with diphenylpyridylphosphine gives first the $H_4Ru_4(CO)_{10}(\mu,\kappa^2$-$Ph_2P$(2-$C_5H_4N$)) cluster (**3**) with a bridging (P,N) coordination of the starting ligand, which easily converts into the phosphide cluster (**4**) at room temperature. The structures of the clusters (**1**)–(**4**) were established using ^{1}H and ^{31}P NMR spectroscopy and X-ray crystallography. Variable temperature ^{1}H NMR study of (**3**) and (**4**) showed that the hydride environment in (**3**) is stereochemically nonrigid and complete exchange of all hydrides was observed at room temperature. The cluster (**4**) exists in solution as an equilibrium mixture of two isomers with different disposition of hydrides relative to the bridging pyridylphosphide moiety.

Keywords: Cluster compounds; P Ligands; Ruthenium; Osmium; X-ray diffraction

1. Introduction

Reactions of pyridylphosphines with ruthenium, rhodium and osmium clusters were studied in detail because of the versatile coordination chemistry of these ligands on the polymetal centers [1–11], which includes oxidative P–C bond cleavage to give the face-bridging pyridylphosphide and formation of either σ-phenyl or bridging pyridyl or benzoyl moieties derived from the starting phosphine [10,12–14]. It is well known that σ-bonded (M–C) organic ligands can be easily removed from coordination sphere of transition metal complexes by reductive coupling with adjacent *cis*-hydride. This classic type of reactions evidently occurs on the treatment of the nonhydride Ru_3 benzoyl containing clusters with dihydrogen [15], $[BH_4]^-$ [15] or PPh_2H [16]. Similar reactivity patterns were also observed for the clusters containing η^1-phenyl provided that a source of hydride was introduced in the reaction mixture [17–20]. In all these cases the reductive elimination is so kinetically and thermodynamically favorable that it was impossible to observe the intermediate hydride cluster. On the contrary, a series of mono- and binuclear transition metal complexes containing hydride and alkyl (aryl)

* Corresponding author. Tel.: +7 812 4284028; fax: +7 812 4286939.
E-mail address: stunik@chem.spbu.ru (S.P. Tunik).
[1] Department of Chemistry, 6-331 Massachusetts Institute of Technology, 77 Massachusetts Ave. Cambridge, MA 02139, USA.

0022-328X/$ - see front matter © 2005 Elsevier B.V. All rights reserved.
doi:10.1016/j.jorganchem.2005.08.007

ligands were isolated and studied in detail because of their importance for understanding the mechanisms of catalytic activation of the hydrocarbon C–H bond, see for example [21–32]. Some particularly stable *cis* "hydride-aryl" complexes of ruthenium [33], iridium [34–36], platinum–tungsten [37] dimers, [Me_2Si]-*ansa*-bridged permethylmetallocene systems [22,24,38] allowed X-ray crystallographic study. In the present paper we report the $H_2Os_3(CO)_{10}$ and $H_4Ru_4(CO)_{12}$ reactions with diphenylpyridylphosphine under various conditions and structural characterization of four novel products formed in these reactions. The $(\mu\text{-H})_2Os_3(CO)_8(\mu_3,\kappa^2\text{-PhPPy})(Ph)$ (**1**) cluster is the first fully characterized hydride cluster containing *cis* hydride and phenyl ligands, which reductively eliminate benzene only under rather harsh conditions.

2. Results and discussion

The reactions of diphenylpyridylphosphine with $H_2Os_3(CO)_{10}$ and $Os_3(CO)_{10}(NCMe)_2$ occurring at progressively increased temperature are shown in Scheme 1, which summarizes the chemistry studied in the present paper and the data obtained earlier [10].

The room temperature reaction of coordinatively unsaturated $H_2Os_3(CO)_{10}$ cluster with the pyridyl-phosphine ligand immediately gives the addition products $H_2Os_3(CO)_{10}(\kappa^1\text{-}Ph_2P(2\text{-}C_5H_4N))$, which has been characterised by IR and NMR spectroscopy. Its ^{31}P chemical shift fits well to that found earlier for the adduct (2.81 ppm [7]) and the IR characteristics are very close to those revealed for analogous $H_2Os_3(CO)_{10}(\kappa^1\text{-}PR_3)$ clusters [39,40] that testifies in favour of terminal coordination of diphenylpyridylphosphine to one of the osmium atoms bridged by the hydride ligands. Heating of the adduct in boiling hexane for 1.5 h gives $(\mu\text{-H})_2Os_3(CO)_8(\mu_3,\kappa^2\text{-PhP-}(2\text{-}C_5H_4N))(Ph)$ (**1**) together with substantially smaller amount of $(\mu\text{-H})Os_3(CO)_9(\mu_3,\kappa^2\text{-PhP}(2\text{-}C_5H_4N))$ (**2**). The formation of **1** from the above κ^1-adduct occurs through coordination of the pyridyl nitrogen and intramolecular oxidative cleavage/addition of a P–C bond in the

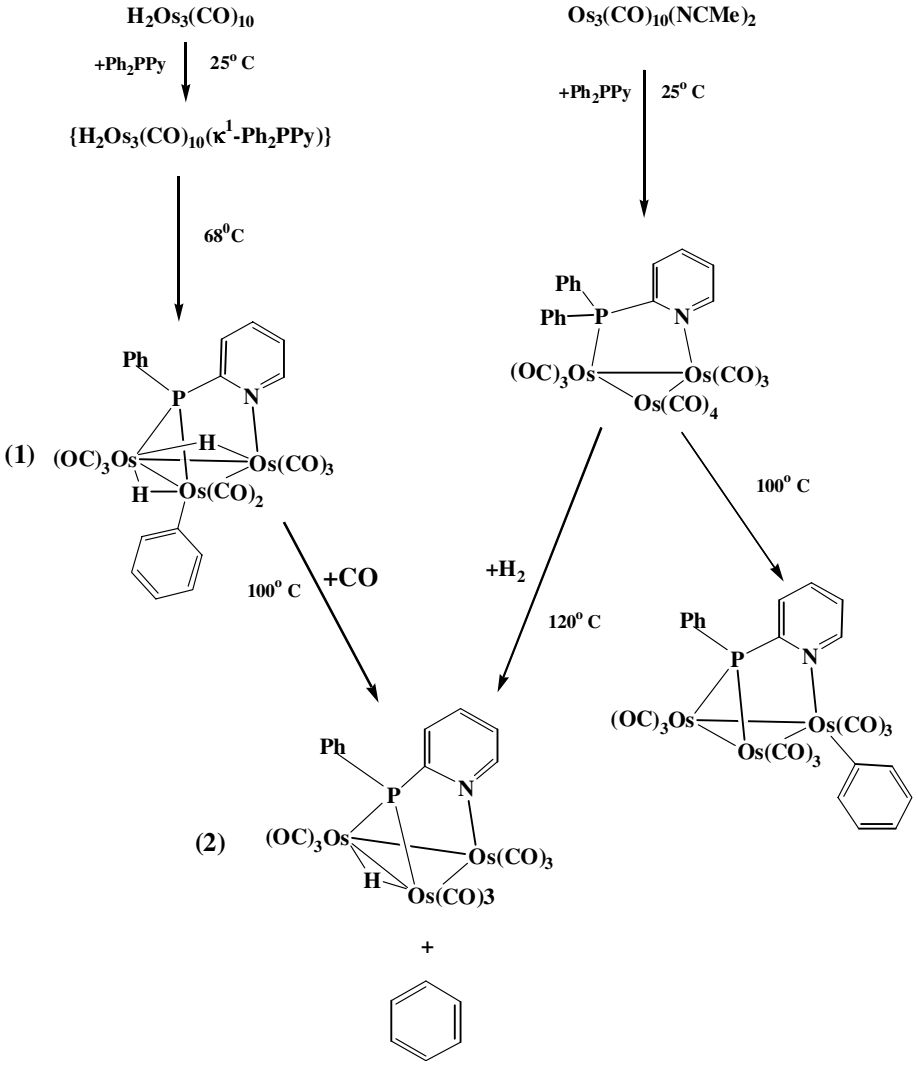

Scheme 1. The reactions of diphenylpyridylphosphine with $H_2Os_3(CO)_{10}$ and $Os_3(CO)_{10}(NCMe)_2$.

coordinated phosphine. These transformations are also accompanied by dissociation of two CO ligands to keep the closed triangular Os_3 framework. The cluster **2** is evidently a result of the further transformation of **1**, which consists of reductive elimination of benzene and reverse addition of a CO ligand to keep 48-electron count of the triangular cluster. Accumulation of benzene in the course of this reaction was detected by proton NMR. It has been also shown independently that gentle heating of **1** in *n*-heptane under CO atmosphere gives **2** in nearly quantitative yield that clearly evidences the left branch of Scheme 1. The same reaction in the absence of CO also gives **2** in slightly lower yield along with accumulation of decomposition products. The observed decomposition is an expectable result under these conditions because some of the starting cluster molecules serve as a source of CO to produce **2**. Molecular structures of **1** and **2** in solid state have been established by X-ray crystallography. ORTEP views of these molecules are shown in Figs. 1 and 2, selected bond lengths and angles are given in Table 2.

Three osmium atoms in **1** form a closed triangle in agreement with 48 electron count for this cluster. The cluster framework is surrounded by eight terminal CO ligands, two bridging hydrides, η^1-coordinated phenyl radical and phenylphosphidopyridyl moiety, which bridges the osmium triangle in nearly symmetric manner. The phenyl ligand occupies a terminal position at the Os(2) atom *cis* to the bridging phosphorus as it should be expected for the coordinated fragments formed through the oxidative addition of the "P–Ph" moiety. This stereochemistry is very much different of that observed in the main product, $Os_3(CO)_9(\mu_3,\kappa^2\text{-PhP}(2\text{-}C_5H_4N))(Ph)$, obtained upon heating of the nonhydride $Os_3(CO)_{10}(\mu,\kappa^2\text{-}Ph_2P(2\text{-}C_5H_4N))$ cluster in heptane solution (98 °C) for 4 h [10]. The metallated phenyl radical in $Os_3(CO)_9(\mu_3,\kappa^2\text{-PhP}(2\text{-}C_5H_4N))(Ph)$ is

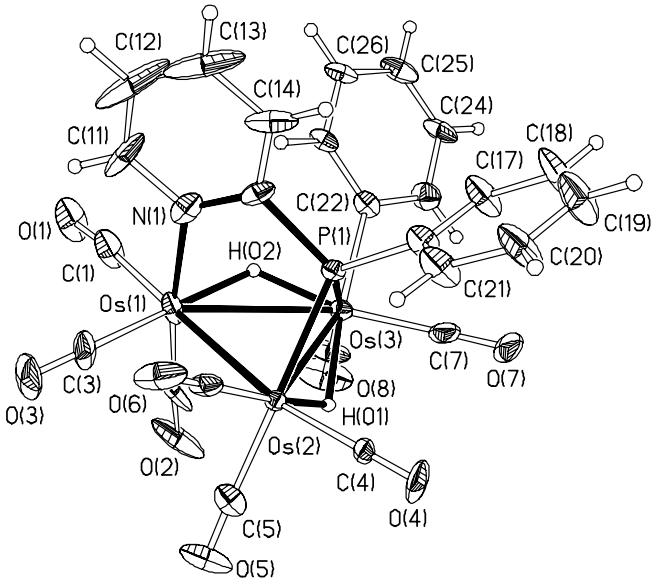

Fig. 1. ORTEP views of the **1** molecule. Thermal ellipsoids are drawn at 50% probability level.

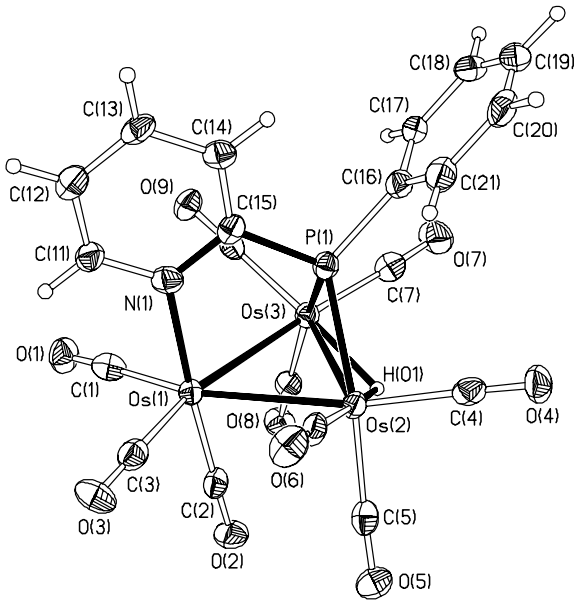

Fig. 2. ORTEP views of the **2** molecule. Thermal ellipsoids are drawn at 50% probability level.

coordinated to the nitrogen bound osmium atom that is a result of the oxidative addition followed by the phenyl group migration across the Os(P-bound)–Os(N-bound) bond. It is worth mentioning that among the products separated from this reaction mixture the authors [10] revealed the $Os_3(CO)_9(\mu_3,\kappa^2\text{-PhP}(2\text{-}C_5H_4N))(\mu\text{-C(O)Ph})$ cluster containing bridging benzoyl ligand, which spans the Os–Os edge bridged by the phosphide group. This means that in the transformation of the unobservable *cis*-(phenyl-phosphide) intermediate the CO migratory insertion into the Os–Ph bond competes with the intermetallic phenyl ligand shift, the latter being either kinetically and/or thermodynamically favourable.

The Os–Os bond lengths in **1** fall in the interval typical for the closed triosmium cluster frameworks. Two of these bonds spanned by the hydride ligands are substantially longer (2.9992(5) and 2.9539(4) Å) compared to the third one (2.8354(4) Å). It has to be noted that in the nonhydride congener of **1**, $Os_3(CO)_9(Ph)(\mu_3,\kappa^2\text{-PhP}(2\text{-}C_5H_4N))$ [10], the Os–Os bond bridged by the phosphido group is the shortest one (2.791 Å) in the molecule due to the effect of bridging phosphorus atom. The presence of a hydride on the same edge of **1** results in a dramatic elongation of this bond up to 2.9539(4) Å. This trend is typical for the phosphido triosmium clusters containing bridging hydrides [41–48] and can be used to reliably locate the hydride position on the clusters framework. The osmium–phosphorus bond lengths in **1** are very close to each other, see Table 2, and very similar to the values (2.344 and 2.338 Å) found in the analogous nonhydride $Os_3(CO)_9(\mu_3,\kappa^2\text{-PhP}(2\text{-}C_5H_4N))(Ph)$ cluster [10]. The Os(1)–N(1) bond is slightly shorter (ca. 0.06 Å) compared to the corresponding distance in the pyridylphosphide triosmium clusters mentioned above [10]. The Os–C distances for the carbonyl

ligands in **1** are very close to each other, except Os(1)–C(2) and Os(2)–C(5), see Table 2. The latter bonds are substantially longer due to pronounced *trans* influence of the phosphide ligand. Two bridging hydrides were located from the difference Fourier map. They occupy the bridging positions over the Os(2)–Os(3) and Os(1)–Os(3) edges that has been also confirmed by the ^{1}H NMR measurements. The hydrides appear in the proton NMR spectrum at −12.30 ppm (d, $J_{P-H} = 5.8$ Hz) and −17.03 ppm (d, $J_{P-H} = 8.0$ Hz) that is typical of bridging coordination mode of these ligands. It is evidently sensible to assign the low field signal in the spectrum of **1** to H(02) and the high field resonance to H(01) taking into account the chemical shift of the hydride ligand in **2** (−18.10 ppm, d, $J_{P-H} = 14.3$ Hz). The values of spin–spin coupling constants for these signals are similar to those found for *cis* stereochemistry of the phosphide phosphorus and proton nuclei [41,42,45,47]. No hydride dynamics was observed in **1** at ambient temperature. The low field part of the spectrum consists of four multiplets (8.86 ppm, d, $J = 5.5$ Hz, H_6; 7.64 ppm, dd, $J = 5.7$, 3.6 Hz, H_4; 7.03 ppm, ddd $J = 5.7$, 5.5, 1.2 Hz, H_5; 6.47 ppm, dd, $J = 3.6$, 7.5 Hz, H_3) corresponding to the pyridyl protons and of the complex phenyl multiplet (10 H) centred at 7.4 ppm. The position and multiplicity of the pyridyl proton signals are in excellent agreement with the data obtained earlier for Ru_3 and Os_3 pyridyl-phosphide clusters [10,14]. The proton and phosphorus NMR data obtained for **1** indicate that the structure found in the solid state remains unchanged in solution.

Reductive elimination of benzene from **1** occurs spontaneously at the temperature above +50 °C, but smooth and nearly quantitative conversion of **1** into **2** was observed at 100 °C in the heptane solution under CO atmosphere. The presence of CO in the reaction mixture substantially facilitate reductive elimination because carbonyl ligand is a stoichiometric reagent in this process and it is also well known that reductive elimination equilibrium is right shifted by the presence of a substituting ligand, which fills the coordination vacancy formed upon elimination. The metal framework in **2** adopts closed triangular configuration in accord with the 48-electron count for this cluster. Nine terminal COs (three at each osmium atom), one bridging hydride and μ_3,κ^2-phenylpyridylphosphide surround the osmium triangle. The molecule adopts C_s symmetry with the mirror plane through Os(1), N(1) and P(1) atoms. Main structural parameters of the metal framework and ligand environment in **2** are essentially similar to those found in **1**, see Table 2. The Os(2)–Os(3) bond bridged by the hydride and phosphido group is the longest one (2.9289(5) Å), the other metal–metal distances are substantially shorter, 2.8528(5) and 2.8384(5) Å. As mentioned above this structural feature can be effectively used to locate the hydride position in the molecules of this sort in addition to the calculations made with the use of XHYDEX program [49]. The NMR measurements confirmed the structure found in the solid state. The hydride signal (−18.1 ppm) appeared in the area typical for the bridging hydrides in triosmium clusters. The signal is splitted into a doublet ($^2J_{P-H} = 14.3$ Hz) due to the interaction with the bridging phosphorus. The phenyl multiplet around 7.5 ppm and four typical signals of coordinated pyridyl protons (9.04, 7.73, 7.07 and 6.34 ppm) are observed in the lowfield area of the proton spectrum.

It was revealed earlier [10] (see Scheme 1) that $Os_3(CO)_{10}(NCMe)_2$ reacts with $Ph_2P(2\text{-}C_5H_4N)$ to give first $Os_3(CO)_{10}(\mu_2,\kappa^2\text{-}Ph_2P(2\text{-}C_5H_4N))$. Thermal treatment of this cluster in boiling heptane results in oxidative addition of a P–Ph moiety to afford the phosphido $Os_3(CO)_9(\mu_3,\kappa^2\text{-}PhP(2\text{-}C_5H_4N))(Ph)$ cluster. We found that under an atmosphere of H_2 the $Os_3(CO)_{10}(\mu_2,\kappa^2\text{-}Ph_2P(2\text{-}C_5H_4N))$ cluster smoothly give **2** in 64% yield. This reaction proceeds through oxidative addition of dihydrogen but the intermediate phenyl-hydride species **1** was not observed due to fast reductive elimination under these conditions.

Scheme 1 comprises essential features of coordination chemistry of diphenylpyridylphosphine in two labile triosmium clusters – $H_2Os_3(CO)_{10}$ and $Os_3(CO)_{10}(NCMe)_2$. Fast coordination of the ligand to the both labile species and further oxidative cleavage of a P–C bond afford trinuclear clusters containing μ_3,κ^2-phosphido and η^1-phenyl ligands. The most interesting finding of the present study is unusual stability of the phenyl-hydrido cluster **1**, which allowed its isolation and full characterization in the solid state and in solution. Intermediacy of the species of this sort is a common point of the mechanistic schemes describing stoichiometric reductive elimination and related catalytic processes. That's why considerable attention has been already paid to investigation of this chemistry and structural characterization of the isolable species, which belong to the family of mono- and binuclear transition metal complexes [22,24,33–38]. However, **1** is the first example of cluster molecule containing *cis*-(R–M–H) fragment, which is stable in the solid state and solution under ambient conditions. Unexpectedly low reactivity of **1** can be partly explained by stereochemical rigidity of the hydrides, which do not display any dynamics at room temperature. Relatively high activation barrier for the hydrides intermetallic scrambling is very likely related to the lack of their reactivity. Necessity to compensate elctronic and coordinative unsaturation arising from reductive elimination of the R–H moiety calls for the presence of a substituting ligand to right-shift the reaction equilibrium. The absence of a two-electron donor in the reaction mixture also retards the reductive elimination and stabilizes **1**.

For the sake of comparison we also studied reactions of another hydride cluster, $H_4Ru_4(CO)_{12}$ with diphenylpyridylphosphine. Direct thermal reaction of these reagents proved to be ineffective to give only minor conversion of the starting cluster. However, a low temperature reaction in the presence of trimethylamine N-oxide followed by gentle heating of the dichloromethane solution gave $H_4Ru_4(CO)_{10}(\mu,\kappa^2\text{-}Ph_2P(2\text{-}C_5H_4N))$ (**3**) (39%) and $H_3Ru_4(CO)_{10}(\mu_3,\kappa^2\text{-}PhP(2\text{-}C_5H_4N))$ (**4**) (7%). The reaction products have been chromatographically separated and

characterized spectroscopically. Solid state structures of both clusters were determined crystallographically, ORTEP views of these molecules are shown in Figs. 3 and 4, selected bond lengths and angles are given in Table 3. The cluster **3** is a typical example of the bridging (P,N) coordination of pyridylphosphine. As in the other polynuclear compounds of this sort [2–11] the pyridylphosphine bridge spans an edge of the metal polyhedron to form the five membered (Ru–P–C–N–Ru) dimetallacycle. Four ruthenium atoms in **3** form a closed tetrahedral framework in accord with the PSEPT rules, which gives 60 electrons count for this cluster. Ten CO ligands together with the phosphorus and nitrogen functionalities of the pyridylphosphine ligand occupy twelve terminal sites, three at each ruthenium atom, in a manner similar to that found in the osmium analogue $H_4Os_4(CO)_{10}(\mu,\kappa^2\text{-}Ph_2P(C_5H_4N))$ [4]. The pyridylphosphine moiety bridges one of two Ru–Ru bond, which are not spanned by the hydrides, to form the dimetallacycle perpendicular to the Ru(1)–Ru(2)–Ru(3) triangle. The "Ru_3(P,N)" structural fragment is a planar chiral [11] unit, the both *S* and *R* configurations of which being presented in the crystal cell. Metal–metal distances in **3** can be divided into two groups, one of which contains four long Ru–Ru bonds spanned by bridging hydrides. Two other Ru–Ru distances are substantially shorter (ca 0.15 Å, see Table 3), the trend being absolutely general for the parent $H_4Ru_4(CO)_{12}$ cluster [50] and its substituted derivatives [51–53] containing bridging ligands. The Ru(1)–Ru(2) bond bridged by the pyridylphosphine moiety is the shortest one in **3** that is evidently a result of the short bite angle of the PN bridging ligand. Configuration and principal geometric parameters (bond length and angles) of the "Ru_3(μ-P,N)" fragment are very similar to those found for the analogous clusters containing the second and third row transition metals [2–4,6,9–11] in this structural unit. In these clusters, as well as in **3**, disparity of the rather long metal–metal bonds and short bite angle of the (P,N) ligand results a strained coordination mode of the bridging moiety. In particular, the Ru(1)–Ru(2)–P(1) angles is quite small (82.4°) compared to the corresponding *cis* angles for the nonstrained CO ligands (90–96°) and the Ru–N–C–P–Ru dimetallacycle in **3** is nonplanar with the Ru(1)–N(1)–C(32)–P(1) and Ru(2)–P(1)–C(32)–N(1) angles equal to 17.1° and 37.5°, respectively. On the contrary, the "Co_2(diphenylpyridylphosphine)" bridge in the cobalt containing polynuclear complexes [5,7,8] is substantially lesser strained due to better match between the ligand bite angle and shorter Co–Co bond that is indicated by nearly planar conformations of the dimetallacycles.

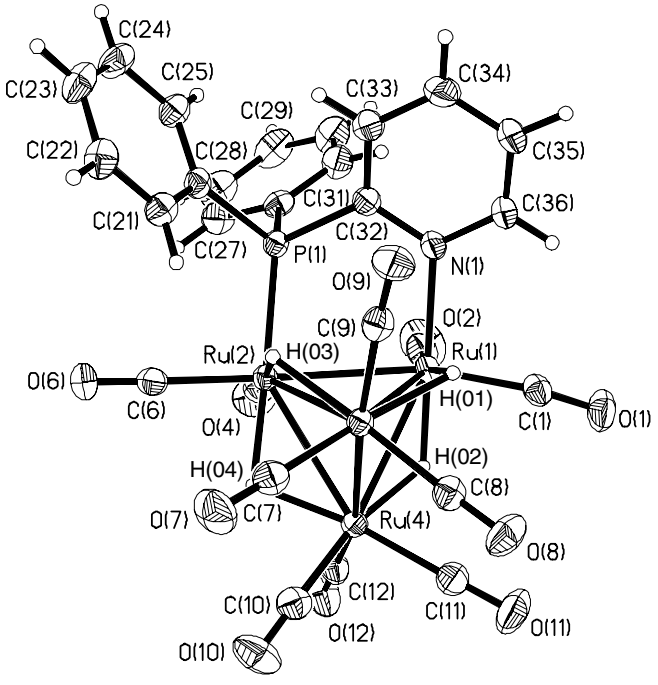

Fig. 3. ORTEP views of the **3** molecule Thermal ellipsoids are drawn at 50% probability level.

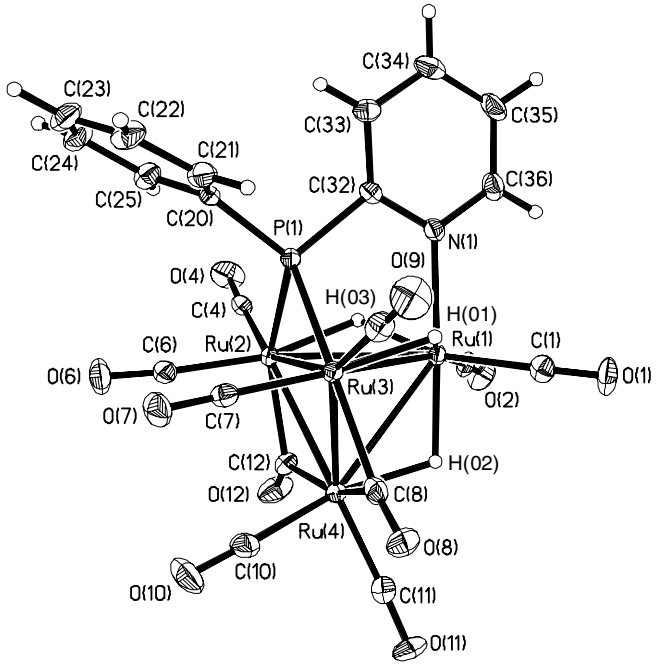

Fig. 4. ORTEP views of the **4** molecule. Thermal ellipsoids are drawn at 50% probability level.

Four hydride ligands in **3** have been located from a difference Fourier map. The arrangement of the hydrides around the Ru_4 framework is exactly the same as that found in the osmium analogue [4] of **3** and was not distorted (compared to $H_4Ru_4(CO)_{12}$) by the substitution of two COs for pyridylphosphine. Two of the hydrides bridge the Ru–Ru bonds *trans* to the phosphorus and nitrogen atoms of the pyridylphosphine moiety. Two others occupy bridging positions on the triruthenium face perpendicular to the dimetallacycle. It is interesting to note that the disposition of the hydrides in **3** differs substantially of that observed in the bridging diphosphine substituted derivatives of $H_4Ru_4(CO)_{12}$ [51–54]. In the diphosphine substituted clusters three of the four hydrides symmetrically bridge

the tetrahedron face perpendicular to the "Ru_3(P,P)" fragment, whereas the fourth occupies a *trans* position relative to one of the phosphorus atoms. The difference in the design of the hydrides environment for the P,P and P,N substituted $H_4Ru_4(CO)_{12}$ derivatives is an evident consequence of the pyridyl functionality "ligand effect", which ought to be mentioned but can be hardly rationalized on the basis of the present knowledge in this field of cluster chemistry.

In line with the chemistry described above and other examples of pyridylphosphines reactions with the nonhydride Ru_3 [12–14] and Os_3 [10] clusters we found that coordinated $Ph_2P(2\text{-}C_5H_4N)$ easily breaks a P–C bond to afford the phosphide $H_3Ru_4(CO)_{10}(\mu_3,\kappa^2\text{-}PhP(2\text{-}C_5H_4N))$ cluster (**4**). The stoichiometry of **4** clearly indicates that this is a product of reductive elimination of benzene from **3**, which occurs under very mild conditions compared to the **1** → **2** transformation. This prevented observation of a phenylhydride intermediate because of a very low barrier to the H–Ph reductive elimination. This situation looks very similar to immediate elimination of benzene or benzaldehyde from the nonhydride $Ru_3(\mu\text{-}C(O)Ph)(\mu_3,\kappa^2\text{-}PhP(2\text{-}C_5H_4N))(CO)_9$ [15] upon their treatment with H_2, $[BH_4]^-$ or $HPPh_2$. Formation of this intermediate containing oxidatively added phenyl moiety is well supported by the results obtained for analogous reactions of the nonhydride Ru_3 clusters [12–15]. It is worth noting that the reaction with $[BH_4]^-$ occurs at room temperature with immediate release of benzaldehyde. These observations indicate that the coordination of the hydride to the ruthenium cluster core (in one or another way) is the limiting stage of the process followed by fast CO insertion and reductive elimination of benzaldehyde.

The molecule of **4**, Fig. 4, consists of a closed (60 electrons) ruthenium tetrahedron surrounded by eight terminal CO, two bridging carbonyls, three hydrides and μ_3,κ^2 coordinated $\{PhP(C_5H_4N)\}$ phosphide ligand. This structural pattern possesses a symmetry plane through the Ru(1), N(1) and P(1) atoms that makes the molecule achiral. The metal–metal bond length in the ruthenium tetrahedron display regular trends typical for the other substituted $H_4Ru_4(CO)_{12}$ substituted clusters. The Ru–Ru bonds bridged by the hydrides are the longest ones (2.9358(3), 2.9385(3), 2.9772(3) Å), the Ru–Ru bond spanned by the phosphide is slightly shorter (2.8712(3) Å), whereas the carbonyl bridged Ru(2)–Ru(4) (2.7398(3) Å) and Ru(3)–Ru(4) (2.7512(3) Å) bonds are the shortest in the molecule. Coordination of the phosphide phosphorus to Ru(2) and Ru(3) atoms in **4** is nearly symmetric and the corresponding bonds length (2.2872(8) and 2.3070(8) Å, respectively) are very close to the Ru–P distance found in **3**. The Ru(1) to N(1) bond length also remains nearly unchanged. Two of the carbonyl ligands in **4** occupy bridging positions on the Ru(2)Ru(4) and Ru(3)Ru(4) edges. The bridging COs are coordinated in a strongly asymmetric manner (Table 3), that does not match C_S symmetry group of the molecule and is most probably dictated by the crystal packing effects.

3. Solution structure and dynamics of the hydride ligands in 3 and 4

The VT proton NMR spectrum of **3** demonstrates the hydride ligands dynamics above −40 °C, Fig. 5. At the low temperature limit (−50 °C) the spectrum in the hydride area displays four signals that is in agreement with the asymmetric structure of the hydride environment. Two of the signals (−14.47 and −23.15 ppm) are not splitted by magnetic interaction with the phosphorus nucleus whereas two others (−16.17 ppm, $^2J_{P-H} = 21.7$ Hz) and (−16.31 ppm, $^2J_{P-H} = 17.2$ Hz) appear as clearly resolved doublets. These NMR data are consistent with the structure of the "H_4Ru_4PN" fragment found in the solid state. Assignment of the hydride signals compatible with this structure is also shown in Fig. 5. The difference between $^2J_{P-H}$ coupling constants for H(03) and H(04) hydrides is completely consistent with their *cis* and *trans* disposition with respect to the phosphorus atom of the ligand, P(1)–Ru(2)–H angles equal 80.6° and 177.9°, respectively. Two other (H(01) and H(02)) hydrides are three bonds separated from the phosphorus nucleus and their signals do not display P–H couplings. The signals of the hydrides ligands simultaneously start to broaden above −40 °C that points to the exchange process(es) involving all hydrides.

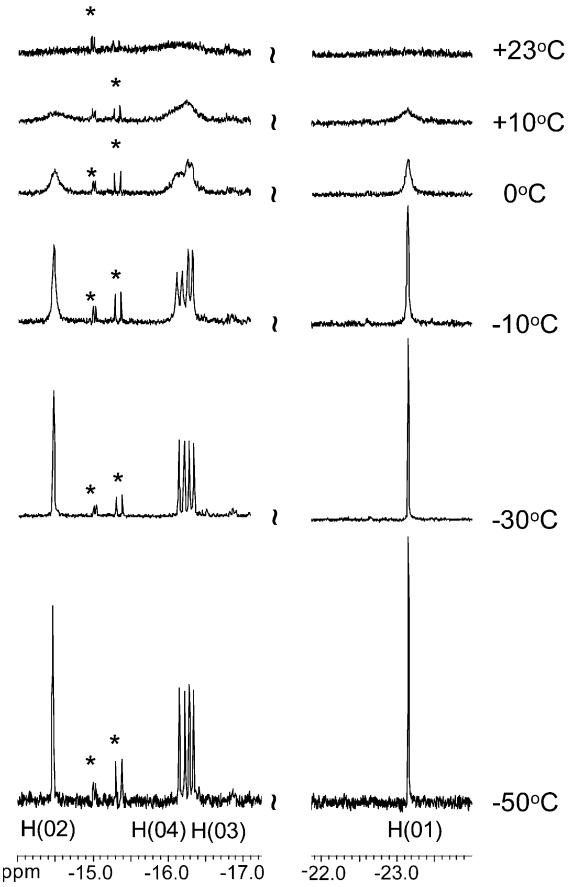

Fig. 5. The VT ^{1}H NMR spectrum of **3**, signals of impurities are marked with asterisks.

The EXSY spectrum run at −30 °C (Fig. S1, Supporting Information) indicates that all hydrides exchange with each other at nearly equal rate.

The limiting low temperature ^{1}H NMR spectrum of **4**, Fig. 6, indicates that this cluster exists in solution as a mixture of two isomers. The signals of the isomers in the hydride area are well resolved and can be interpreted on the basis of spin–spin coupling constants observed in each of the spectroscopic patterns. The major isomer displays two signals in 2/1 ratio. The low field resonance of double intensity is splitted into a doublet with a typical *cis* $^2J_{P-H}$ equal to 8.8 Hz, whereas the high field signal appears as a singlet. These observations are in agreement with the structure of the "Ru_4H_3P" fragment revealed in the solid state and plausible spin–spin couplings in this system. The spectrum of the minor isomer consists of three signals of single intensity, two of which appear in the close vicinity to the low field signal of the major isomer and the chemical shift of the third one is very close to that of the high field resonance of the major species. This is indicative of completely asymmetric structure of the "Ru_4H_3P" fragment in the minor isomer. Two low field signals display spin–spin coupling constants equal to 17.7 and 10.3 Hz that points to two bond coupling of the corresponding hydrides to the phosphorus nucleus. The most probable structure compatible with the position of these signals and their couplings to phosphorus is shown in Scheme 2. In this structure the hydride, which occupy the Ru(1)–Ru(4) edge appears in the spectrum as a singlet at −22.74 ppm. This is the only bridging position on the ruthenium tetrahedron, which prevents coupling with the phosphide phosphorus that makes this assignment unambiguous. Two low field doublets of the minor isomer display different $^2J_{P-H}$ couplings, one of which (−18.10 ppm) is very close (10.3 Hz) to the value observed in the doublet signal of the major species (8.8 Hz). It is therefore sensible to assign this signal to the hydride occupying the Ru–Ru edge spanned by the P–C–N bridge that puts the phosphorus and the hydride into *cis* position. The other doublet signal (−17.68 ppm) displays substantially higher phosphorus to hydride coupling (17.7 Hz) that very probably correspond to nearly *trans* disposition of the intervening nuclei as shown in Scheme 2. Heating of the solution of **4** up to +23 °C results in averaging of the low field and high field resonances of the isomers to give two broad signals at −17.40 and −23.10 ppm, respectively (Fig. 6). This observation indicates that in the temperature range studied there is an exchange between major and minor isomers, which may be also accompanied by intramolecular hydrides scrambling.

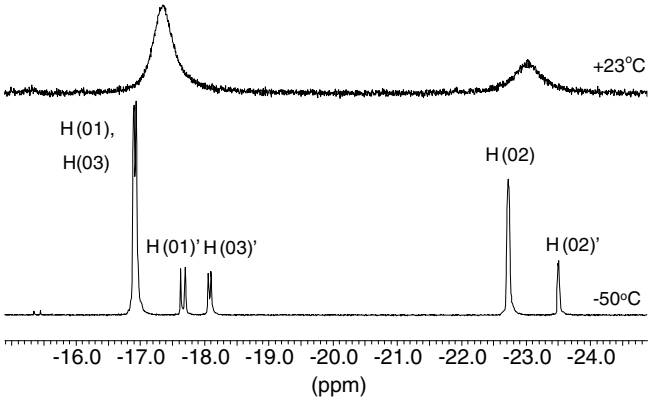

Fig. 6. The limiting low temperature and room temperature ^{1}H NMR spectra of **4**. Signals of minor isomer are marked with apostrophe.

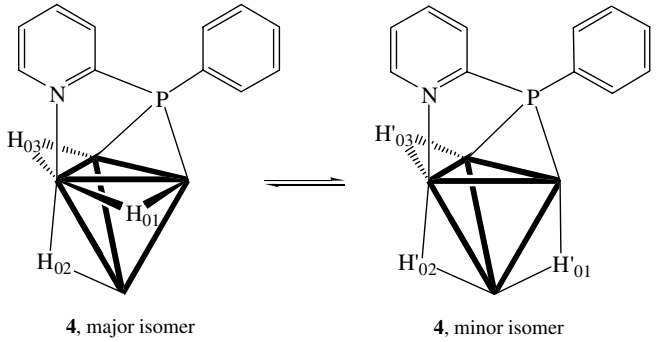

Scheme 2. Exchange of hydrides in **4**.

4. Experimental

The following reagents were purchased commercially and purified prior to use: diphenyl-2-pyridylphosphine (Aldrich) was recrystallized from hot methanol; $Ru_3(CO)_{12}$ (Aldrich) was recrystallized from hot benzene; trimethylamine N-oxide (Aldrich) was sublimed in vacuo. The triosmium $H_2Os_3(CO)_{10}$ [55], $Os_3(CO)_{10}Ph_2P(2\text{-}C_5H_4N)$ [10] and tetraruthenium $H_4Ru_4(CO)_{12}$ [56] clusters were synthesized according to published procedures. Reagent grade solvents: petroleum ether (40–70 °C), methanol, dichloromethane and hexane were distilled over appropriate drying agents prior to use. Analytical TLC, used for monitoring of the reaction course, was carried out on Merck aluminum sheets coated with 0.5 mm silica gel 60. The products were purified by column chromatography on Silica (5–40 mesh). The IR spectra were recorded on a Specord M80 spectrometer. Mass spectra were measured on an MX-1321 instrument (electron impact, ionizing potential 70 eV). The ^{1}H and ^{31}P NMR spectra were recorded on a Bruker DX 300 spectrometer. The chemical shifts were referenced to residual solvent resonances and external 85% H_3PO_4 in the ^{1}H and ^{31}P spectra, respectively. Microanalyses were carried out in the Analytical Laboratories of the University of Joensuu, Osaka-City University and St. Petersburg State University.

4.1. Reaction of $H_2Os_3(CO)_{10}$ and $Ph_2P(2\text{-}C_5H_4N)$

$Ph_2P(2\text{-}C_5H_4N)$ (46.4 mg, 0.176 mmol) was dissolved in 20 ml of hexane and $H_2Os_3(CO)_{10}$ (150.8 mg, 0.176 mmol) was added to this solution under vigorous stirring. Formation of the $H_2Os_3(CO)_{10}(\kappa^1\text{-}PPh_2(2\text{-}C_5H_4N))$ adduct was

evidenced by precipitation of yellow solid and decoloration of the starting dark violet solution. The adduct was decanted and washed with hexane (177 mg, 0.159 mmol, 89.9%). IR (CH_2Cl_2, cm^{-1}): ν(CO) 2105w, 2065m, 2048m, 2022vs, 1976sh. $^{31}P\{^1H\}$ NMR (121 MHz, $CDCl_3$, 25 °C) $\delta = 3.7$ ($^1J_{Os-P} = 203$ Hz, 1P).

4.2. Synthesis of $(\mu\text{-}H)_2Os_3(CO)_8(\mu_3,\kappa^2\text{-}PhP(2\text{-}C_5H_4N))(Ph)$

85 mg (0.0761 mmol) $H_2Os_3(CO)_{10}(\kappa^1\text{-}PPh_2(2\text{-}C_5H_4N)$ was dissolved in 30 cm^3 of hot hexane and refluxed for 1.5 h. The color of solution turned from yellow to dark-brown. Evaporation of the solvent in vacuo gave brown solid material. It was dissolved in CH_2Cl_2 (0.7 cm^3), diluted with hexane (1.5 cm^3) and transferred onto a chromatographic column (2.5 × 6 cm). Elution with CH_2Cl_2/petroleum ether (1/1, v/v) gave trace amounts of $Os_3(CO)_{12}$, yellow band of $(\mu\text{-}H)Os_3(CO)_9(\mu_3,\kappa^2\text{-}PhP(2\text{-}C_5H_4N))$ (**2**) (12.3 mg, 0.012 mmol, 16%) and yellow-brown band of $(\mu\text{-}H)_2Os_3(CO)_8(\mu_3,\kappa^2\text{-}PhPPy)(Ph)$ (**1**) (36 mg, 0.034 mmol, 44%).

(**1**) IR (CH_2Cl_2, cm^{-1}): ν(CO) 2085s, 2049vs, 2022vs, 2004m, 1996m, 1960m. ^1H NMR (300 MHz, $CDCl_3$, 25 °C) $\delta = 8.86$ (d, $J = 5.5$ Hz, 1H, H_6 Py), 7.64 (dd, $J = 5.7$, 3.6 Hz, 1H, H_4 Py), 7.03 (ddd, $J = 5.7$, 5.5, 1.2 Hz, 1H, H_5 Py), 6.47 (dd, $J = 3.6$, 7.5 Hz, 1H, H_3 Py), 7.60–7.30, (m, 10H, Ph–P and Ph–Os), −12.2 (d, $J_{P-H} = 6.57$ Hz, 1H, OsH), −16.63 (d, $J_{P-H} = 7.28$ Hz, 1H, OsH), $^{31}P\{^1H\}$ NMR (121 MHz, $CDCl_3$, 25 °C) $\delta = 20.0$ (s, 1P). Due to thermal instability of **1** its mass spectrum displays the highest m/z signal corresponding to elimination of C_6H_6 – ($M^+ - C_6H_6$) 1013 ($Os_3 = 570$) followed by fragmentation of a few COs: ($M^+ - C_6H_6 - n$CO), $n = 1$–4. Anal. calc. for $C_{25}H_{16}N_1O_8Os_3P_1$ (1060.06): C, 28.33; H, 1.52; N, 1.32. Found: C, 28.41; H, 1.48; N, 1.16%. Single crystals of **1** suitable for an X-ray analysis were grown from CH_2Cl_2/hexane mixture at 2 °C.

(**2**) IR (CH_2Cl_2, cm^{-1}): ν(CO) 2081m, 2051vs, 2025s, 1998m, 1978m, 1946sh. ^1H NMR (300 MHz, $CDCl_3$, 25 °C) $\delta = 9.04$ (d, $J = 5.5$ Hz, 1H, H_6 Py), 7.73 (dd, $J = 5.5$, 3.7 Hz, 1H, H_4 Py), 7.05 (m, $J = 6.4$ Hz, 1H, H_5 Py), 6.34 (dd, $J = 7.3$, 3.7 Hz, 1H, H_3 Py), 7.5–7.4 (m, 5H, Ph–P), −18.1 (d, $J_{P-H} = 14.3$ Hz, 1H, OsH). $^{31}P\{^1H\}$ NMR (121 MHz, $CDCl_3$, 25 °C) $\delta = 19.2$ ($^1J_{Os-P} = 115$ Hz). MS (m/z): M^+ 1013($Os_3 = 570$) followed by fragmentation of four COs: ($M^+ - n$CO), $n = 1$–4. Anal. calcd. for $C_{20}H_{10}N_1O_9Os_3P_1$ (1009.96): C, 23.78; H, 1.00; N, 1.39. Found: C, 24.48; H, 1.01; N, 1.30%. Single crystals of **2** suitable for an X-ray analysis were grown from hexane at 2 °C.

4.3. Reaction of the $Os_3(CO)_{10}(\mu,\kappa^2\text{-}Ph2P(2\text{-}C_5H_4N))$ cluster with dihydrogen

$Os_3(CO)_{10}(\mu,\kappa^2\text{-}Ph_2P(2\text{-}C_5H_4N)$ (31.1 mg, 0.030 mmol) was dissolved in octane (30 ml) and H_2 was bubbled through the reaction mixture under reflux for 24 h. The solvent was then removed in vacuo to give yellow solid material which was dissolved in 0.5 cm^3 of CH_2Cl_2, diluted wit 1 cm^3 hexane and separated by column (2.5 × 4 cm) chromatography with petroleum ether/CH_2Cl_2 (1/1, v/v). $(\mu\text{-}H)Os_3(CO)_9$ ($\mu_3,\kappa^2\text{-}PhP(2\text{-}C_5H_4N)$) (**2**) (18 mg, 0.018 mmol, 63.7%) was obtained as the main product of this reaction.

4.4. Thermal conversion of $(\mu\text{-}H)_2Os_3(CO)_8(\mu_3,\kappa^2\text{-}PhP(2\text{-}C_5H_4N))(Ph)$ (**1**) into $(\mu\text{-}H)Os_3(CO)_9(\mu_3,\kappa^2\text{-}PhP(2\text{-}C_5H_4N))$ (**2**)

10.3 mg $(\mu\text{-}H)_2Os_3(CO)_8(\mu_3,\kappa^2\text{-}PhP(2\text{-}C_5H_4N))(Ph)$ (**1**) was dissolved in 20 cm^3 of heptane and the solution was purged with CO. The reaction mixture was then refluxed for 15 min under constant flow of gaseous CO. TLS spot test showed complete conversion of **1** into **2**. The solvent than was removed in vacuo to give yellow solid material. The ^1H NMR spectrum of the material obtained showed nearly quantitative (ca 90%) conversion of **1** into **2**. A similar experiment carried out in $CDCl_3$ solution unambiguously showed reductive elimination of benzene by emerging of a sharp resonance at 7.37 ppm in the proton NMR spectrum.

4.5. Reaction of $H_4Ru_4(CO)_{12}$ with $Ph_2P(2\text{-}C_5H_4N)$

$H_4Ru_4(CO)_{12}$ (75 mg, 0.101 mmol) and $Ph_2P(2\text{-}C_5H_4N)$ (26.5 mg, 0.101 mmol) were dissolved in 20 ml of CH_2Cl_2. The solution was placed in a Schlenk tube and degassed by three freeze–pump–thaw cycles. Degassed solution of $Me_3NO \cdot 2H_2O$ (24.6 mg, 0.222 mmol) in a CH_3OH/CH_2Cl_2 mixture (0.5/5 ml) was transferred via cannula to the frozen mixture of $H_4Ru_4(CO)_{12}$ and $Ph_2P(2\text{-}C_5H_4N)$. The reaction mixture was allowed to warm up to room temperature under vigorous shaking to give an orange solution. Heating of this mixture to the boiling point for 6–7 times gave the final vinous-red solution. The solution was concentrated under vacuo to 1 ml and transferred onto a silica column (5 × 3.5 cm) with hexane/CH_2Cl_2 (3/2, v/v). Three bands were isolated in the order of elution: wide yellow band $H_4Ru_4(CO)_{12}$; wide brown band $H_4Ru_4(CO)_{10}(\mu,\kappa^2\text{-}Ph_2P(2\text{-}C_5H_4N))$ (**3**) (37.9 mg, 0.040 mmol, 39%), pale-red narrow band of $H_3Ru_4(CO)_{10}(\mu_3,\kappa^2\text{-}PPh(2\text{-}C_5H_4N))$ (**4**) (5.8 mg, 0.007 mmol, 7%).

(**3**): IR (hexane, cm^{-1}), ν(CO) 2085w, 2081s, 2067s, 2058m, 2051m, 2043w, 2028s, 2023s, 2013m, 2009m, 1987m, 1945w. ^1H NMR (300 MHz, $CDCl_3$, −30 °C) $\delta = 9.14$ (d, $J = 5.7$ Hz, 1H, Py), 7.05 (m, 2H, Py), 6.30 (dd, $J = 6.5$, 4.5 Hz, 1H, Py), 7.34–7.75 (m, 10H, Ph), −14.47 (s, 1H, H(01)), −16.17 (d, $J_{P-H} = 21.7$ Hz, 1H, H(04)), −16.31 (d, $J_{P-H} = 17.2$ Hz, 1H, H(03)), −23.15 (s, 1H, H(02)). $^{31}P\{^1H\}$ NMR (121 MHz, $CDCl_3$, 25 °C) $\delta = 25.5$ (s). MS-FAB+ (m/z): 951 (M^+) (calc 951), [M^+–nCO], $n = 1$, 3, 4, 5, 6. Anal calc for **3** + 1/2 C_6H_{14}: $C_{30}H_{25}NO_{10}PRu_4$ C, 36.22; H, 2.53; N, 1.43%. Found: C, 36.46; H, 2.64; N, 1.51%.

(**4**): IR (ν(CO), hexane, cm^{-1}) 2085m, 2081w, 2067w, 2058w, 2051s, 2028m, 2023s, 2014s, 1993m, 1987m, 1945w. The signals of two (major and minor) isomers were found in the ^1H and ^{31}P spectra of **4**.

Major isomer. ^1H NMR (300 MHz, $CDCl_3$, 223 K) $\delta = 8.60$ (d, $J = 5.15$ Hz, 1H, Py), 7.65–7.55 (m, 5H, Ph), 7.50 (d, $J = 6.30$ Hz, 1H, Py), 7.27 (t, $J = 6.40$ Hz, 1H, Py), 6.27 (d, $J = 7.59$ Hz, 1H, Py), −16.94 (d, $^2J_{P-H} = 8.8$ Hz, 2H, H(01) + H(03)), −22.74 (s, 1H, H(02)). ^{31}P NMR (121 MHz, $CDCl_3$, 298 K) $\delta = 118.1$ (s). *Minor isomer*. ^1H NMR (300 MHz, $CDCl_3$, 223 K) $\delta = 8.46$ (d, $J = 5.32$ Hz, 1H, Py), 7.65–7.55 (m, 5H, Ph + 1 H Py), 7.16 (t, $J = 6.40$ Hz, 1H, Py), 6.27 (d, $J = 7.59$ Hz, 1H, Py), −17.68 (d, $J = 17.7$ Hz, 1H, H(01)), −18.10 (d, $J = 10.3$ Hz, 1H, H(03)), −23.50 (d, $J = 3.1$ Hz, 1H, H(02)). ^{31}P NMR (121 MHz, $CDCl_3$, 298 K) $\delta = 122.6$ (s). MS-FAB + (m/z): 874 (M^+) (calc. 874), [$M^+ - n$CO], $n = 1$–3. Anal. calc. for $C_{21}H_{12}NO_{10}PRu_4$: C, 28.87; H, 1.38; N, 1.60. Found: C, 27.44; H, 1.56, N, 1.54%. Single crystals of **3** and **4** were obtained by slow diffusion of hexane into CH_2Cl_2 solutions of these clusters at +5 °C.

4.6. X-ray structure determinations

The crystals of **1** and **2** were immersed in perfluoropolyether, mounted in a cryo-loops and measured at 100 K temperature. The X-ray diffraction data were collected with a Nonius KappaCCD diffractometer using Mo Kα radiation ($\lambda = 0.71073$ Å). The EvalCCD (**1**) or Denzo-Scalepack [57,58] (**2**, **3**, **4**) programs packages were used for cell refinements and data reductions. The structures were solved either by Patterson heavy atom method using the DIRDIF-99 program (**2**, **4**) or by direct methods using the SHELXS-97 program (**1**, **3**) with the WinGX graphical user interface [59–61]. An empirical absorption correction based on equivalent reflections was applied to all data (SADABS v. 2.10 for **1** and XPREP in SHELXTL v. 6.14 for **2**, **3**, **4**) [62,63]. The ratio of minimum to maximum transmissions were 0.4675, 0.4040, and 0.8420 respectively for **1**, **2** and **3**. Structural refinements were carried out with SHELXL-97 [60]. Hydrides in **1** were located from the difference Fourier map but were not refined. The location of the hydride hydrogen (H01) in **2** was determined by XHYDEX program [49]. In **3** the hydride hydrogens were located from a difference Fourier map and refined with fixed Uiso = 0.05. In **4** the hydrides were placed in an idealized position with XHYDEX program [49]. All other hydrogens were placed in idealized positions and constrained to ride

Table 2
Selected bond lengths (Å) and angles (°) for **1** and **2**

	1	**2**
Os(1)–Os(2)	2.8354(4)	2.8528(5)
Os(1)–Os(3)	2.9992(5)	2.8384(5)
Os(2)–Os(3)	2.9539(4)	2.9289(5)
Os(1)–C(2)	1.899(11)	1.892(11)
Os(2)–C(5)	1.930(8)	1.936(12)
Os(1)–N(1)	2.158(7)	2.187(9)
Os(2)–P(1)	2.352(2)	2.342(3)
Os(3)–P(1)	2.337(2)	2.345(3)
N(1)–C(15)	1.340(10)	1.354(13)
P(1)–C(15)	1.810(8)	1.817(10)
Os(1)–Os(2)–Os(3)	62.364(11)	58.786(13)
Os(1)–Os(3)–Os(2)	56.880(10)	59.268(13)
Os(1)–N(1)–C(15)	121.2(5)	119.7(7)
Os(2)–P(1)–C(15)	110.6(3)	115.3(3)
Os(3)–P(1)–C(15)	116.3(2)	113.8(3)
Os(2)–P(1)–Os(3)	78.09(5)	77.33(8)
N(1)–C(15)–P(1)	114.2(6)	112.4(7)

Table 1
Crystallographic data for **1**–**4**

	1	**2**	**3**	**4**
Empirical formula	$C_{25}H_{16}NO_8Os_3P$	$C_{20}H_{10}NO_9Os_3P$	$C_{30}H_{25}NO_{10}PRu_4$	$C_{21}H_{12}NO_{10}PRu_4$
F_w	1059.96	1009.86	994.76	873.57
Temperature (K)	100(2)	100(2)	120(2)	120(2)
λ (Å)	0.71073	0.71073	0.71073	0.71073
Crystal system	Monoclinic	Orthorhombic	Monoclinic	Triclinic
Space group	$P2_1/c$	$Pbca$	$P2_1/c$	$P\bar{1}$
a (Å)	9.9993(8)	15.8704(3)	12.19320(10)	10.3823(1)
b (Å)	16.7951(14)	16.0803(3)	14.4381(2)	10.5342(1)
c (Å)	16.2898(11)	18.5394(4)	20.5163(5)	12.9826(6)
α (°)	90	90	90	76.6072(7)
β (°)	96.854(7)	90	92.3195(5)	69.4710(7)
γ (°)	90	90	90	75.1912(7)
V (Å^3)	2716.1(4)	4731.27(16)	3608.87(11)	1269.65(6)
Z	4	8	4	2
$\rho_{calc.}$ (g/cm^3)	2.592	2.835	1.831	2.285
μ(Mo Kα) (mm^{-1})	14.106	16.192	1.737	2.452
Reflns collected/unique	25455/5524	35014/4643	41460/6875	9519/4920
R_{int}	0.0486	0.0514	0.0334	0.0117
R_1[a] ($I \geqslant 2\sigma$)	0.0312	0.0355	0.0247	0.0204
wR_2[b] ($I \geqslant 2\sigma$)	0.0467	0.0803	0.0653	0.0625

[a] $R_1 = \sum\|F_o| - |F_c\|/\sum|F_o|$.
[b] $wR_2 = [\sum[w(F_o^2 - F_c^2)^2]/\sum[w(F_o^2)^2]]^{1/2}$.

Table 3
Selected bond lengths (Å) and angles (°) for **3** and **4**

	3	4
Ru(1)–Ru(2)	2.7703(4)	2.9385(3)
Ru(1)–Ru(3)	2.9553(4)	2.9358(3)
Ru(1)–Ru(4)	2.9228(4)	2.9772(3)
Ru(2)–Ru(3)	2.9840(4)	2.8712(3)
Ru(2)–Ru(4)	2.8975(4)	2.7398(3)
Ru(3)–Ru(4)	2.7784(4)	2.7512(3)
Ru(1)–N(1)	2.169(3)	2.173(2)
Ru(2)–P(1)	2.2871(9)	2.2872(8)
Ru(3)–P(1)		2.3070(8)
P(1)–C(32)	1.840(3)	1.831(3)
N(1)–C(32)	1.356(4)	1.361(4)
P(1)–C(32)–N(1)	116.0(2)	120.0(2)
C(32)–N(1)–Ru(1)	121.8(2)	120.0(2)
C(32)–P(1)–Ru(2)	114.49(11)	114.26(10)
C(32)–P(1)–Ru(3)		114.04(10)

on their parent atom. In the structure **3**, half a molecule of hexane was found in the asymmetric unit. The solvent molecules were completely disordered around a center of symmetry and the carbons were refined only isotropically with equal displacement parameter. Because of the disorder, hydrogens of the solvent molecule were omitted. The crystallographic data are summarized in Table 1, selected bond lengths and angles are given in Tables 2 and 3.

Acknowledgements

The authors gratefully acknowledge financial support from the Academy of Finland (to M.H. and T.A.P.); the Nordic Council of Ministers (to T.S.P.); Russian Foundation for Basic Research, Grant 05-03-33266 and Humboldt Foundation, Grant V-RKS-RUS/1074525 (for E.V.G.) We also thank the Analytical Laboratory of Material Chemistry Department of the Osaka-City University for CHN analysis of the osmium clusters.

Appendix A. Supplementary data

Supplementary data associated with this article can be found, in the online version, at doi:10.1016/j.jorganchem.2005.08.007.

References

[1] C. Graiff, A. Ienco, C. Massera, C. Mealli, G. Predieri, A. Tiripicchio, F. Ugozzoli, Inorg. Chim. Acta 330 (2002) 95.
[2] C.G. Arena, D. Drommi, F. Faraone, M. Lanfranchi, F. Nicolo, A. Tiripicchio, Organometallics 15 (1996) 3170.
[3] K. Wajda-Hermanowicz, F. Pruchnik, M. Zuber, G. Rusek, E. Galdecka, Z. Galdecki, Inorg. Chim. Acta 232 (1995) 207.
[4] Y.-Y. Choi, W.-T. Wong, J. Organomet. Chem. 573 (1999) 189.
[5] F.-E. Hong, Y.-C. Chang, R.-E. Chang, C.-C. Lin, S.-L. Wang, F.-L. Liao, J. Organomet. Chem. 588 (1999) 160.
[6] J.W.-S. Hui, W.-T. Wong, J. Cluster Sci. 10 (1999) 91.
[7] R. Gobetto, C.G. Arena, D. Drommi, F. Faraone, Inorg. Chim. Acta 248 (1996) 257.
[8] P. Braunstein, C. Graiff, C. Massera, G. Predieri, J. Rose, A. Tiripicchio, Inorg. Chem. 41 (2002) 1372.
[9] A.J. Deeming, M.B. Smith, J. Chem. Soc., Chem. Commun. (1993) 844.
[10] A.J. Deeming, M.B. Smith, J. Chem. Soc., Dalton Trans. (1993) 3383.
[11] S.P. Tunik, I.O. Koshevoy, A.J. Poe, D.H. Farrar, E. Nordlander, M. Haukka, T.A. Pakkanen, Dalton Trans. (2003) 2457.
[12] N. Lugan, G. Lavigne, J.J. Bonnet, Inorg. Chem. 25 (1986) 7.
[13] N. Lugan, G. Lavigne, J.J. Bonnet, Inorg. Chem. 26 (1987) 585.
[14] A.J. Deeming, M.B. Smith, J. Chem. Soc., Dalton Trans. (1993) 2041.
[15] N. Lugan, G. Lavigne, J.J. Bonnet, R. Reau, D. Neibecker, I. Tkatchenko, J. Am. Chem. Soc. 110 (1988) 5369.
[16] N. Lugan, P.L. Fabre, D. de Montauzon, G. Lavigne, J.J. Bonnet, J.Y. Saillard, J.F. Halet, Inorg. Chem. 32 (1993) 1363.
[17] M.P. Cifuentes, M.G. Humphrey, B.W. Skelton, A.H. White, J. Organomet. Chem. 513 (1996) 201.
[18] A.A. Cherkas, J.F. Corrigan, S. Doherty, S.A. MacLaughlin, F. van Gastel, N.J. Taylor, A.J. Carty, Inorg. Chem. 32 (1993) 1662.
[19] F. Van Gastel, A.J. Carty, M.A. Pellinghelli, A. Tiripicchio, E. Sappa, J. Organomet. Chem. 385 (1990) C50.
[20] M. Lanfranchi, A. Tiripicchio, E. Sappa, A.J. Carty, J. Chem. Soc., Dalton Trans. (1986) 2737.
[21] J.-C. Choi, T. Sakakura, J. Am. Chem. Soc. 126 (2003) 7762.
[22] D.G. Churchill, K.E. Janak, J.S. Wittenberg, G. Parkin, J. Am. Chem. Soc. 125 (2003) 1403.
[23] S. Reinartz, P.S. White, M. Brookhart, J.L. Templeton, J. Am. Chem. Soc. 123 (2001) 12724.
[24] H. Lee, B.M. Bridgewater, G. Parkin, Dalton Trans. (2000) 4490.
[25] K.B. Renkema, R. Bosque, W.E. Streib, M. Feliu, O. Eisenstein, K.G. Caulton, J. Am. Chem. Soc. 121 (1999) 10895.
[26] R.A. Stockland Jr., G.K. Anderson, N.P. Rath, J. Am. Chem. Soc. 121 (1999) 7945.
[27] G.P. Rosini, K. Wang, B. Patel, A.S. Goldman, Inorg. Chim. Acta 270 (1998) 537.
[28] A.D. Selmeczy, W.D. Jones, R. Osman, R. Perutz, Organometallics 14 (1995) 5677.
[29] J.F. Hartwig, R.A. Andersen, R.G. Bergman, Organometallics 10 (1991) 1710.
[30] W.D. Jones, V.L. Kuykendall, Inorg. Chem. 30 (1991) 2615.
[31] J.S. Merola, Organometallics 8 (1989) 2975.
[32] W.D. Jones, F.J. Feher, Acc. Chem. Res. (1989) 91.
[33] M. Antberg, L. Dahlenburg, K.-M. Frosin, N. Hock, Chem. Ber. 121 (1988) 859.
[34] W.D. McGhee, R.G. Bergman, J. Am. Chem. Soc. 108 (1986) 5621.
[35] H.E. Selnau, J.S. Merola, Organometallics 12 (1993) 1583.
[36] H. Werner, A. Hohn, M. Dziallas, Angew. Chem. Int., Ed. Engl. 25 (1986) 1090.
[37] A. Albinati, R. Naegeli, A. Togni, L.M. Venanzi, Organometallics 2 (1983) 926.
[38] H. Lee, P.J. Desrosiers, I. Guzei, A.L. Rheingold, G. Parkin, J. Am. Chem. Soc. 120 (1998) 3255.
[39] L.J. Farrugia, J. Organomet. Chem. 394 (1990) 515.
[40] S.P. Tunik, V.D. Khripun, M. Haukka, T.A. Pakkanen, Dalton Trans. (2004) 1775.
[41] A.J. Arce, A.J. Deeming, Y. De Sanctis, A.M. Garcia, J. Manzur, E. Spodine, Organometallics 13 (1994) 3381.
[42] W.R. Cullen, S.J. Rettig, H. Zhang, Inorg. Chim. Acta 251 (1996) 53.
[43] B.F.G. Johnson, J. Lewis, E. Nordlander, P.R. Raithby, C.E. Housecroft, Inorg. Chim. Acta 259 (1997) 345.
[44] S.B. Colbran, P.T. Irele, B.F.G. Johnson, F.J. Lahoz, J. Lewis, P.R. Raithby, J. Chem. Soc., Dalton Trans. (1989) 2023.
[45] A.J. Deeming, S. Doherty, M.W. Day, K.I. Hardcastle, H. Minassian, J. Chem. Soc., Dalton Trans. (1991) 1273.
[46] H.G. Ang, C.H. Koh, L.L. Koh, W.L. Kwik, W.K. Leong, W.Y. Leong, J. Chem. Soc., Dalton Trans. (1993) 847.
[47] A.J. Arce, R. Machado, Y. De Sanctis, T. Gonzalez, R. Atencio, A.J. Deeming, Inorg. Chim. Acta 344 (2003) 123.

[48] W.R. Cullen, S.J. Rettig, T.C. Zheng, Organometallics 12 (1993) 688.
[49] A.G. Orpen, J. Chem. Soc., Dalton Trans. (1980) 2509.
[50] R.D. Wilson, S.M. Wu, R.A. Love, R. Bau, Inorg. Chem. 17 (1978) 1271.
[51] M.I. Bruce, E. Horn, O. Bin Shawkataly, M.R. Snow, E.R.T. Tiekink, M.L. Williams, J. Organomet. Chem. 316 (1986) 187.
[52] M.A. Churchill, R.A. Lashewicz, J.R. Shapley, S.I. Richter, Inorg. Chem. 19 (1980) 1277.
[53] P. Homanen, R. Persson, M. Haukka, T.A. Pakkanen, E. Nordlander, Organometallics 19 (2000) 5568.
[54] S.P. Tunik, T.S. Pilyugina, I.O. Koshevoy, S.I. Selivanov, M. Haukka, T.A. Pakkanen, Organometallics 23 (2004) 568.
[55] H.D. Kaesz, S.A.R. Knox, J.W. Koepke, R.B. Saillant, J. Chem. Soc. D (1971) 477.
[56] S.A.R. Knox, J.W. Koepke, M.A. Andrews, H.D. Kaesz, J. Am. Chem. Soc. 97 (1975) 3942.
[57] Z. Otwinowski, W. Minor, in: R.M. Sweet (Ed.), Processing of X-ray Diffraction Data Collected in Oscillation Mode, vol. 276, Academic Press, 1997, pp. 307–326.
[58] A.J.M. Duisenberg, L.M.J. Kroon-Batenburg, A.M.M. Schreurs, J. Appl. Crystallogr. 36 (2003) 220.
[59] P.T. Beurskens, G. Beurskens, R. de Gelder, S. Garcia-Granda, R.O. Gould, R. Israel, J.M.M. Smits, The DIRDIF-99 program system, Crystallography Laboratory, University of Nijmegen, The Netherlands, 1999.
[60] G.M. Sheldrick, SHELXL97, Program for Crystal Structure Refinement, University of Gottingen, Germany, 1997.
[61] L.J. Farrugia, J. Appl. Crystallogr. 32 (1999) 837.
[62] G.M. Sheldrick, Bruker Analytical X-ray Systems, Bruker AXS Inc., Madison, WI, USA, 2002.
[63] G.M. Sheldrick, Bruker Analytical X-ray Systems, SADABS – Bruker Nonius scaling and absorption correction v 2.10, Bruker AXS Inc., Madison, WI, USA, 2003.